Fragment approach to the electronic structure of τ-boron allotrope

Naiwrit Karmodak and Eluvathingal D. Jemmis[*]

Department of Inorganic and Physical Chemistry, Indian Institute of Science, Bangalore-560012, Karnataka

(Received 19 November 2016; published 19 April 2017)

The presence of nonconventional bonding features is an intriguing part of elemental boron. The recent addition of τ boron to the family of three-dimensional boron allotropes is no exception. We provide an understanding of the electronic structure of τ boron using a fragment molecular approach, where the effect of symmetry reduction on skeletal bands of B_{12} and the B_{57} fragments are examined qualitatively by analyzing the projected density of states of these fragments. In spite of the structural resemblance to β boron, the reduction of symmetry from a rhombohedral space group to the orthorhombic one destabilizes the bands and reduces the electronic requirements. This suggests the presence of the partially occupied boron sites, as seen for a β boron unit cell, and draws the possibility for the existence of different energetically similar polymorphs. τ boron has a lower binding energy than β boron.

I. INTRODUCTION

The structure, stability, and variety of boron allotropes have been long debated [1–15]. While the controversy associated with the stability of α-vs β-rhombohedral boron allotrope is yet to be solved [4,6,12,16,17], the discovery of τ boron put forth another challenge [18]. The analysis of a β-rhombohedral boron sample using high-resolution transmission electron microscopy (HRTEM) indicated the presence of grains belonging to this new phase [18]. Though this form is built up of similar fragments as the β-rhombohedral boron, the computations reported that τ boron is more stable than other allotropic forms [18]. Here, we present a detailed structural overview and an explanation for the varying electron requirement of the B_{57} fragment of the τ boron allotrope based on a fragment molecular approach [19–21]. We also report the relative stability of α, β, γ, and τ boron using density functional computations and conclude that β-rhombohedral boron is the most stable. The varying electron requirements of the two allotropes are accounted for by using the mno rule [6]. According to this, m+n+o is the number of electron pairs required for stabilizing the condensed polyhedral boranes or the constituent fragments of boron allotropes, where m is the number of polyhedral units, n the number of vertices and o the number of singly shared boron atoms (details in Supplemental Material [22]).

II. THE STRUCTURE OF τ BORON ALLOTROPE

The structure of τ boron allotrope is based on icosahedral B_{12} units and B_{57} units. Figures 1(a) and 1(b) show a simple view of the idealized primitive unit cell of τ boron, where the complex structural fragments are modeled as spheres of varying sizes. Each idealized orthorhombic unit cell with *Cmcm* space group contains eight B_{12} units and two B_{28}-B-B_{28} units, rounding to 210 boron atoms. The smallest yellow sphere denotes the single boron atom connecting two B_{28} fragments (larger purple spheres). The eight icosahedral B_{12} units are denoted by medium-sized blue, red, and green

spheres. Figures 1(c) and 1(d) show the real overview of the unit cell, where the arrangements of the B_{12} units and B_{28}-B-B_{28} units are depicted. The green icosahedral units with C_{2h} symmetry occupy the eight vertices and the longest edges of the orthorhombic unit cell [Fig. 1(c)]. The blue and red icosahedral units are present within the unit cell and have C_s and C_{2v} symmetry, respectively. Two B_{57} units (B_{28}-B-B_{28}) are oriented along the vertical axis of the unit cell, connecting the B_{12} units among each other [Fig. 1(d)]. The arrangements of the icosahedral units and the B_{57} unit in β-rhombohedral boron are shown in Figs. 1(e), 1(f), and 1(g). Thirty-five nonequivalent boron atoms are present in τ boron (β-B_{105} has 15). The quantum mechanical calculations show that removal of one boron atom (B13, orange spheres) from the B_{57} units as shown in Fig. 2 and addition of an extra four boron atoms enhances the stability of this form [18]. Thus the unit cell with 212 boron atoms (denoted as τ-B_{106}) is found to be more favorable in comparison to an idealized unit cell (B_{210}, denoted as τ-B_{105}). An increase of binding energy by the addition of extra atoms is also seen for β-B_{106} previously, where the idealized unit cell has only 105 atoms [6,7,14,21]. Figure 1(h) gives a comparative overview of the arrangement for the constituent fragments in β and τ boron allotrope. The zigzag orientation of the B_{57} units in τ boron doubles the unit-cell size with respect to β boron.

III. COMPUTATIONAL DETAILS

The relative energies for the four three-dimensional (3D) allotropes of boron are computed at two different density functionals as PW91 [23] and Perdew-Burke-Ernzerhof (PBE) [24], using the Vienna *ab initio* simulation package (VASP) [25–28], with plane-wave basis set having an energy cutoff of 600 eV and an equivalent set of k-point grids with spacing of around $2\pi \times 0.02$ Å^{-1}. The projector augmented wave pseudopotentials [29,30] are implemented to treat the electron-ion interactions. The electronic energy convergence threshold is set to 10^{-6} eV in energy and 10^{-3} eV/Å for force. The zero-point energy (ZPE) corrections are done using a finite displacement method [31] with a displacement amplitude of around 0.05 Å, using the PHONOPY code [32].
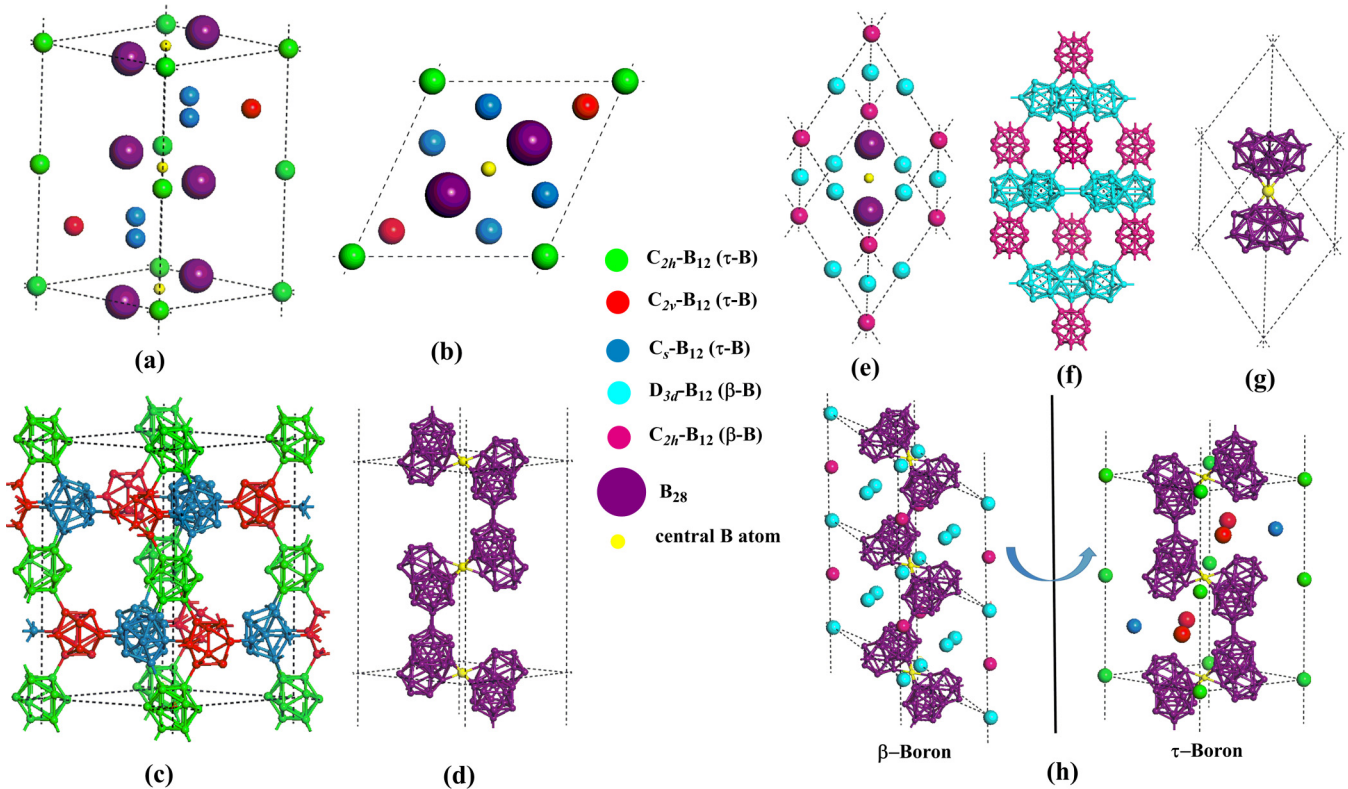
---

[*]jemmis@ipc.iisc.ernet.in

Legend:
- C_{2h}-B_{12} (τ-B) — green
- C_{2v}-B_{12} (τ-B) — red
- C_s-B_{12} (τ-B) — blue
- D_{3d}-B_{12} (β-B) — cyan
- C_{2h}-B_{12} (β-B) — pink
- B_{28} — purple
- central B atom — yellow

FIG. 1. The arrangement of the B_{12} units and the B_{28}-B-B_{28} units in the τ-B_{105} (a–d) and β-B_{105} (e–g) unit cells. (a) Simplified side view of the unit cell. (b) Top view of the unit cell. (c) The arrangement of B_{12} units within the unit cell. The different types of the icosahedral units are denoted by different colors. (d) Arrangement of B_{28}-B-B_{28} units along the central axis of the unit cell. (e) A simplified view of the β-B_{105} unit cell. (f) The arrangement of the icosahedral units in the idealized unit cell of β-B_{105}. (g) The orientation of B_{28}-B-B_{28} fragments in β-B_{105}. (h) The structural comparison of the β- vs τ-boron allotrope. The spheres denote the B_{12} units present within the unit cell.

IV. RESULTS AND DISCUSSION

Unlike the previous report [18], in our hands the PW91 gives β-B_{106} to be the most stable allotopic form without addition of ZPE correction. The τ-B_{106} is found to be less stable by 13.8 meV/atom. Relative energies of α-B_{12} and γ-B_{28} allotrope are higher than β-B_{106} by 2.4 and 29.4 meV/atom. The α-B_{12} allotrope is computed to be lower in energy than the β-B_{106} by 0.7 meV/atom using the PBE functional. Addition of the ZPE correction reorganizes the ordering and makes the β-B_{106} the most stable. The ZPE values for α-B_{12} and β-B_{106} are found to be 131.75 and 128.34 meV/atom, respectively. These ZPE values are in good agreement with the previously calculated values [18]. However, the τ-B_{106} is less stable than both the

α- and β-B_{106}, with and without ZPE correction. The ZPE values for the β-B_{106} and τ-B_{106} are almost similar, since the constituting fragments are the same. The γ-boron allotrope remains the least stable among the four allotropes at all levels (Table I).

The reduction in symmetry of the icosahedral B_{12} units in τ-B_{106} allotrope in comparison to the β-B_{106} unit cell has a dramatic consequence. The local symmetry of B_{12} units is reduced from those in the β-B_{106} (D_{3d} at the vertices and C_{2h} at edge centers) to a C_{2h}, C_{2v}, and C_s point group in τ-B_{106}. Figure 3 shows a qualitative orbital correlation diagram depicting the effect on the molecular orbitals of individual B_{12} units upon distortion from ideal I_h symmetry when it forms a part of the β and τ boron allotropes. The I_h in Fig. 3(a) denotes the I_h-$B_{12}H_{12}{}^{-2}$. Other B_{12} structures, denoted as (b)–(f) in Fig. 3, are obtained by defragmenting the B_{12}
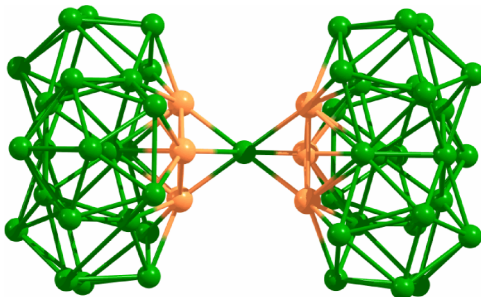

FIG. 2. The B_{28}-B-B_{28} fragment of a β-rhombohedral unit cell. Here six orange spheres denote the B13 boron atoms.

TABLE I. The relative differences in the energy values for the four most stable allotropic forms of boron calculated at two different DFT functionals. The energy values are reported with respect to the β-B_{106} structure in meV/atom.

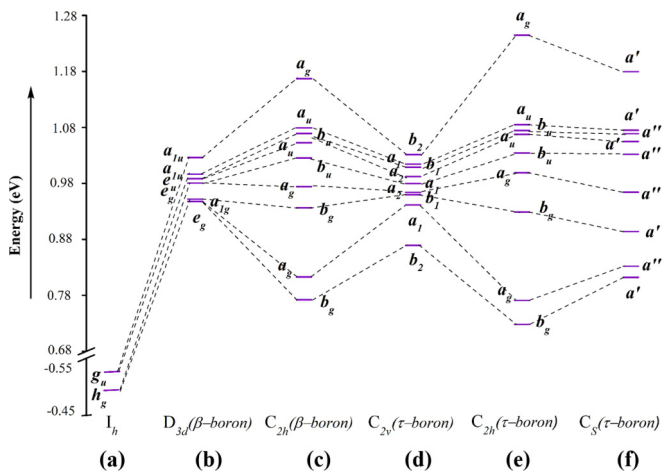| DFT functionals	α-B_{12}	β-B_{106}	τ-B_{106}	γ-B_{28}
PW91 (without ZPE)	2.4	0.0	13.8	29.4
PBE (without ZPE)	−0.7	0.0	11.8	26.4
PBE (with ZPE)	2.71	0.0	11.8	25.1

FIG. 3. The orbital correlation diagram between the highest occupied orbitals of ideal icosahedral $B_{12}H_{12}^{-2}$ and the B_{12} fragments taken out of the β and τ allotropes after saturating with 12 H atoms: (a) I_h-$B_{12}H_{12}^{-2}$, (b) and (c) D_{3d} and C_{2h} B_{12} fragments in β boron; (d), (e), and (f) denotes the C_{2v}, C_{2h}, and C_s B_{12} units in τ boron, respectively. The correlation diagram is computed using a GAUSSIAN 09 [33] package at the PBE/SVP [34–36] level of theory.

units from the β boron and τ boron allotrope. The dangling valences are satisfied with H atoms, and extra dinegative charges are provided to calculate the orbital arrangement in these fragments. The lowering of symmetry from I_h to D_{3d} in the β boron destabilizes the frontier skeletal orbitals (h_g and g_u) and splits into doubly degenerate and singly degenerate levels. Upon further reduction of symmetry to C_{2h} [Fig. 3(c)], the doubly degenerate orbitals are split into nondegenerate ones, whereas the other skeletal orbitals undergo slight reorganization such that a few levels are stabilized and a few are destabilized. The distortion of symmetry for the individual B_{12} fragments in τ boron has similar consequences. While the C_{2v} distortion stabilizes these frontier orbitals to some extent with respect to the D_{3d} and C_{2h} symmetry in β boron, the deformation corresponding to C_{2h} and C_s symmetry has both a stabilizing and destabilizing effect on the orbitals. However, a considerable change in the energy ordering is not observed for these molecular fragments as compared to D_{3d} and C_{2h} symmetry in β boron.

In order to visualize the effect of change in unit-cell symmetry from rhombohedral to orthorhombic on the constituent fragments, the projected density of states (PDOS) for the bands corresponding to the B_{12} units in β-B_{105} and τ-B_{105} is plotted (Fig. 4). Figure 4(a) represents the PDOS plot for β-B_{105}, where the bands denoted by the black region correspond to the B_{12} units present at the vertices [pink B_{12} units in Fig. 1(e)], whereas the red region corresponds to the B_{12} units at the edge centers [blue B_{12} units in Fig. 1(e)]. In τ-B_{105}, three types of icosahedral units are present as denoted by green, blue, and red spheres in Fig. 1(a). The states denoted by the black region in the PDOS plot [Fig. 4(b)] belong to the green icosahedral units, the red region represents the red B_{12} units, and the blue region denotes the bands belonging to blue B_{12} units. In comparison to β-B_{105}, the corresponding peaks are broadened over the entire energy range. This is due to the splitting of the bands

of icosahedral B_{12} units upon reduction of the symmetry in τ boron. A few levels are destabilized and move above the Fermi level [indicated by an arrow in Fig. 4(b)]; however, the arrangement of the electronic levels are almost similar for the B_{12} units in both the phases (β-B_{105} and τ-B_{105}). Though the arrangement of the bands corresponding to these B_{12} units in both the allotropes could not be correlated directly with that seen for the individual $B_{12}H_{12}^{-2}$ units in Fig. 3, it gives a qualitative explanation for the effect of change in symmetry on the B_{12} bands upon moving from a β-rhombohedral to τ-orthorhombic unit cell. Figures 4(c) and 4(d) represent the PDOS plot for the B_{57} fragments of β-B_{105} and τ-B_{105}, respectively. The density of states corresponding to the frontier occupied levels of the B_{57} units in β-B_{105} is more compared to the vacant levels present above the Fermi region [marked as arrows in Fig. 4(c)]. But in τ-B_{106}, the ordering changes, which increases the density of states for the vacant states above the Fermi levels compared to the filled states present below the Fermi region. This shows that the electronic requirement of the B_{57} units in τ-B_{105} must be less as compared to the β-B_{105}.

As per the electron counting rules [6,37–40], the eight B_{12} units need 16 electrons and the two B_{57} units together should be provided with $+6$ charge. Thus An *et al.* removed one boron atom (B13) from each B_{57} unit, which is equivalent to removing three electrons, and added an extra four boron atoms, equivalent to adding 12 electrons, resulting in the τ-B_{106} [18]. This must enhance the cohesive energy per atom of the system. However, a greater charge transfer from the B_{57} units to B_{12} units, as seen in the variation of density of states (Fig. 4), signifies a decrease of the electronic requirement of the B_{57} fragments in τ-B_{105} compared to β-B_{105}. Thus, in order to estimate the electronic requirement of these fragments, we have designed a few model structures for τ boron starting from ideal τ-B_{105} and compared the relative cohesive energy per atom with the reported τ-B_{106} structure in Table II. Fragments involved in those structures are also shown in Table II. The structures denoted as τ-B_{105}(a), τ-$B_{105.5}$(a), τ-B_{106}(a), and τ-$B_{106.5}$(a) are obtained in the following way. One B13 boron atom from both the B_{57} fragments of the idealized unit cell B_{210} of τ boron is removed to give B_{208} (two B_{27}-B-B_{28} and eight B_{12}). Addition of two to six extra boron atoms to this unit cell provides τ-B_{105}(a), τ-$B_{105.5}$(a), τ-B_{106}(a), τ-$B_{106.5}$(a), and τ-B_{107}(a), respectively. Here τ-B_{106}(a) is the same structure reported by An *et al.* [18]. The removal of another B13 boron atom from one of the B_{56} fragments results in B_{27}-B-B_{27}, leading to the other set of structures denoted as τ-B_{105}(b), τ-$B_{105.5}$(b), and τ-B_{106}(b). Here formally three to five extra boron atoms are added to the B_{207} (B_{27}-B-B_{27} + B_{27}-B-B_{28} + $8B_{12}$) unit cell. Since ZPE corrections would be similar for these polymorphic structures, due to the presence of identical constituting fragments, energy values are reported without ZPE corrections. Structures which follow the mno rule, i.e., the ones with one boron removed from the B_{28}-B-B_{28} unit, is in general more stable. The removal of another boron atom from the B_{56} entity subtracts three more electrons from the system, which is equivalent to a B_{57} unit with six positive charges. Though our computations indicate that the B_{57} units in τ-B_{105} can accommodate a greater formal positive charge, in comparison to that in
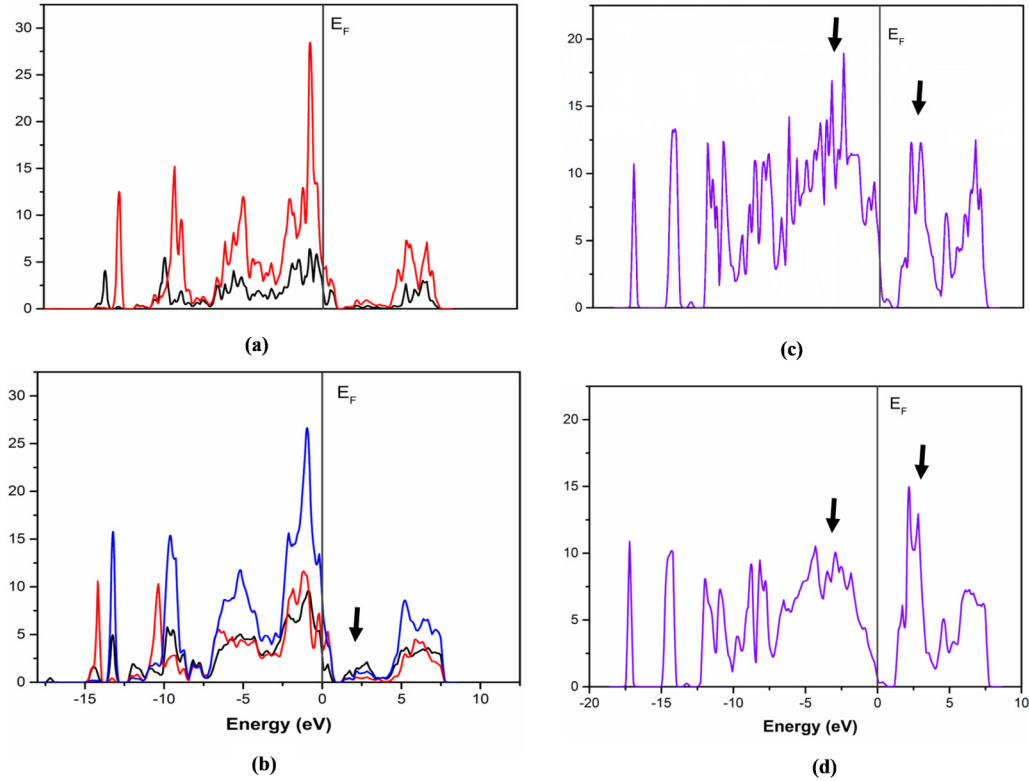
FIG. 4. The projected density of states for the β-B_{105} and τ-B_{105}. (a) Represents the bands corresponding to B_{12} units in β-B_{105}. The black region corresponds to pink B_{12} units and the red region to light blue B_{12} units in Fig. 1(e). (b) The PDOS plot of the B_{12} units present in τ-B_{105}. Here the black region denotes the green B_{12} units, the red region corresponds to the red B_{12} units, and the blue region to the blue B_{12} units in Fig. 1(a); (c) and (d) show the PDOS plot for the B_{57} units in β-B_{105} and τ-B_{105}, respectively. The arrows are shown to indicate the changes observed for the PDOS plot in τ boron in comparison to β boron.

β-B_{105}, removal of six electrons might result in removing a greater number of electrons than required. This reduces the stability of the polymorphs containing this fragment. The

TABLE II. Relative energy values (R.E.) at the PBE level with respect to β-B_{106} for the different polymorphic structures of τ boron obtained from the idealized τ-B_{105} unit cell. The constituting fragments are indicated, and N denotes the number of boron atoms per unit cell. The letter (a) in column 1 refers to those structures containing two B_{56} fragments and eight B_{12} units, whereas letter (b) refers those structures containing one B_{56}, one B_{55}, and eight B_{12} units.

Formula	Fragments	N	R.E. (meV/atom)
β-B_{106}	$B_{56} + 4B_{12} + 2B$	106	0.0
τ-B_{105}	$2B_{57} + 8B_{12}$	210	25.8
τ-B_{105}(a)	$2B_{56} + 8B_{12} + 2B$	210	18.1
τ-B_{105}(b)	$B_{56} + B_{55} + 8B_{12} + 3B$	210	17.5
τ-$B_{105.5}$(a)	$2B_{56} + 8B_{12} + 3B$	211	11.9
τ-$B_{105.5}$(b)	$B_{56} + B_{55} + 8B_{12} + 4B$	211	13.9
τ-B_{106}(a)[a]	$2B_{56} + 8B_{12} + 4B$	212	11.8
τ-B_{106}(b)	$B_{56} + B_{55} + 8B_{12} + 5B$	212	14.7
τ-$B_{106.5}$(a)	$2B_{56} + 8B_{12} + 5B$	213	11.5
τ-B_{107}(a)	$2B_{56} + 8B_{12} + 6B$	214	26.7

[a]This structure is equivalent to the τ-B_{106} structure already reported by An *et al.* [18].

cohesive energy per boron atom is a nearly constant value for τ-$B_{105.5}$(a), τ-B_{106}(a), and τ-$B_{106.5}$(a). It is worth pointing out, however, that there is only one possibility to satisfy the electron count of B_{12} units in a near perfect fashion, given that the B_{57} units require a $+3$ charge or its equivalent B_{56}. This is τ-$B_{106.5}$(a), which has 15 electrons (instead of the 16 required) around 8 B_{12}, which is lower in energy than the τ-B_{106}(a) reported earlier [18]. Addition of another boron atom would give 18 electrons in place of the needed 16 and is not more stable, as seen by the approximate model τ-B_{107}(a).

Thus the addition of 12–15 electrons per idealized unit cell of τ boron is sufficient. However, the relative stability of all the structures is less than that of β-B_{106} (Table II). This is due to the slight destabilization of the bands corresponding to constituent fragments upon reduction of symmetry in τ boron [Figs. 4(b) and 4(d)]. In structural terms this destabilization corresponds to the strain introduced by the twisting of B_{28}-B-B_{28} in the chain [Fig. 1(h)]. These consequences also point out that in comparison to the β boron phase [1,12,41], a greater number of boron atoms should have partial occupancies in τ boron. The presence of partially occupied boron atoms would reduce the electron density of the system and lead to the existence of several polymorphs with almost equivalent stability and a different number of boron atoms per unit cell. The trend in relative energy values shown in Table II validates this argument. This is reminiscent of the structure of β boron, where the extra occupancies and vacancies depend on the rate of cooling of the boron melt, resulting in several closely related

structures. Obviously, several such strains are anticipated in any experimental attempt to crystallize boron.

V. CONCLUSIONS

We found that due to the reduction of symmetry, the electronic requirement of the constituent fragments in τ-B_{105} is reduced as compared to β-B_{105}. The skeletal bands become split and push a few bands above the Fermi level, reducing its relative stability slightly in the process. Reduction of the electronic requirement indicates the presence of partially occupied boron sites and stems out for the possible existence of other polymorphic structures of this new allotrope with varying atomic densities. The density functional theory (DFT) results also show that the predicted structure for τ boron is less stable than that of the β boron structure.

Note added. While this article was under review, two Comments on Ref. [18] by Werheit and by Ogitsu *et al.* and an Erratum appeared. Werheit argued that the twined structure of τ boron arises due to the mechanical processing of the β-boron sample [42]. An *et al.* responded that twinning is uniformly distributed in the grain, and therefore is not the cause of mechanical stress applied during the processing of a sample [43]. They also pointed out that inconsistent use of pseudopotentials had led them to conclude initially that τ boron is more stable than β boron [18]. Ogitsu *et al.* showed that τ boron is not the ground state of boron, as is shown here as well [44]. This was reiterated by An *et al.* in an erratum which also showed that the most stable B13 sites are similar to that in beta-rhombohedral boron as shown by us earlier in a fragment analysis [45,6].

[1] J. L. Hoard, D. B. Sullenger, C. H. L. Kennard, and R. E. Hughes, J. Solid State Chem. **1**, 268 (1970).

[2] J. L. Hoard and R. E. Hughes, in *The Chemistry of Boron and Its Compounds*, edited by E. L. Muetterites (Wiley, New York, 1967).

[3] B. F. Decker and J. S. Kasper, Acta Crystallogr. **12**, 503 (1959).

[4] B. Albert and H. Hillebrecht, Angew. Chem., Int. Ed. **48**, 8640 (2009).

[5] S. Aydin and M. Simsek, J. Alloys Compd. **509**, 5219 (2011).

[6] E. D. Jemmis and M. M. Balakrishnarajan, J. Am. Chem. Soc. **123**, 4324 (2001).

[7] E. D. Jemmis and D. L. V. K. Prasad, Curr. Sci. **95**, 1277 (2008).

[8] A. R. Oganov *et al.*, Nature (London) **457**, 863 (2009).

[9] A. R. Oganov, V. L. Solozhenko, C. Gatti, O. O. Kurakevych, and Y. Le Godec, J. Superhard Mater. **33**, 363 (2011).

[10] T. Ogitsu, F. Gygi, J. Reed, M. Udagawa, Y. Motome, E. Schwegler, and G. Galli, Phys. Rev. B **81**, 020102 (2010).

[11] T. Ogitsu and E. Schwegler, Solid State Sci. **14**, 1598 (2012).

[12] T. Ogitsu, E. Schwegler, and G. Galli, Chem. Rev. **113**, 3425 (2013).

[13] K. Shirai, H. Dekura, Y. Mori, Y. Fujii, H. Hyodo, and K. Kimura, J. Phys. Soc. Jpn. **80**, 084601 (2011).

[14] M. J. van Setten, M. A. Uijttewaal, G. A. de Wijs, and R. A. de Groot, J. Am. Chem. Soc. **129**, 2458 (2007).

[15] M. A. White, A. B. Cerqueira, C. A. Whitman, M. B. Johnson, and T. Ogitsu, Angew. Chem. **127**, 3697 (2015).

[16] M. Widom and M. Mihalkovič, Phys. Rev. B **77**, 064113 (2008).

[17] M. Widom and M. Mihalkovič, J. Phys.: Conf. Ser. **176**, 012024 (2009).

[18] Q. An, K. M. Reddy, K. Y. Xie, K. J. Hemker, and W. A. Goddard, Phys. Rev. Lett. **117**, 085501 (2016).

[19] M. M. Balakrishnarajan, P. D. Pancharatna, and R. Hoffmann, New J. Chem. **31**, 473 (2007).

[20] E. Jemmis and M. Balakrishnarajan, Bull. Mater. Sci. **22**, 863 (1999).

[21] D. L. V. K. Prasad, M. M. Balakrishnarajan, and E. D. Jemmis, Phys. Rev. B **72**, 195102 (2005).

[22] See Supplemental Material at http://link.aps.org/supplemental/10.1103/PhysRevB.95.165128 for a detailed description of mno rule and its application to estimate the electron requirements of β and τ boron allotrope.

[23] J. P. Perdew, J. A. Chevary, S. H. Vosko, K. A. Jackson, M. R. Pederson, D. J. Singh, and C. Fiolhais, Phys. Rev. B **46**, 6671 (1992).

[24] J. P. Perdew, K. Burke, and M. Ernzerhof, Phys. Rev. Lett. **77**, 3865 (1996).

[25] G. Kresse and J. Hafner, Phys. Rev. B **48**, 13115 (1993).

[26] G. Kresse and J. Furthmüller, Comput. Mater. Sci. **6**, 15 (1996).

[27] G. Kresse and J. Furthmüller, Phys. Rev. B **54**, 11169 (1996).

[28] G. Kresse and J. Hafner, Phys. Rev. B **49**, 14251 (1994).

[29] G. Kresse and D. Joubert, Phys. Rev. B **59**, 1758 (1999).

[30] P. E. Blöchl, Phys. Rev. B **50**, 17953 (1994).

[31] G. Kresse, J. Furthmüller, and J. Hafner, Europhys. Lett. **32**, 729 (1995).

[32] A. Togo and I. Tanaka, Scr. Mater. **108**, 1 (2015).

[33] M. J. Frisch, G. W. Trucks, H. B. Schlegel, G. E. Scuseria, M. A. Robb, J. R. Cheeseman, G. Scalmani, V. Barone, B. Mennucci, G. A. Petersson, H. Nakatsuji, M. Caricato, X. Li, H. P. Hratchian, A. F. Izmaylov, J. Bloino, G. Zheng, J. L. Sonnenberg, M. Hada, M. Ehara, K. Toyota, R. Fukuda, J. Hasegawa, M. Ishida, T. Nakajima, Y. Honda, O. Kitao, H. Nakai, T. Vreven, J. A. Montgomery, Jr., J. E. Peralta, F. Ogliaro, M. Bearpark, J. J. Heyd, E. Brothers, K. N. Kudin, V. N. Staroverov, R. Kobayashi, J. Normand, K. Raghavachari, A. Rendell, J. C. Burant, S. S. Iyengar, J. Tomasi, M. Cossi, N. Rega, J. M. Millam, M. Klene, J. E. Knox, J. B. Cross, V. Bakken, C. Adamo, J. Jaramillo, R. Gomperts, R. E. Stratmann, O. Yazyev, A. J. Austin, R. Cammi, C. Pomelli, J. W. Ochterski, R. L. Martin, K. Morokuma, V. G. Zakrzewski, G. A. Voth, P. Salvador, J. J. Dannenberg, S. Dapprich, A. D. Daniels, Ö.

Farkas, J. B. Foresman, J. V. Ortiz, J. Cioslowski, and D. J. Fox, Gaussian 09, Revision E.01 (Gaussian, Inc., Wallingford, CT, 2009).

[34] A. Schäfer, H. Horn, and R. Ahlrichs, J. Chem. Phys. **97**, 2571 (1992).

[35] A. Schäfer, C. Huber, and R. Ahlrichs, J. Chem. Phys. **100**, 5829 (1994).

[36] F. Weigend and R. Ahlrichs, Phys. Chem. Chem. Phys. **7**, 3297 (2005).

[37] K. Wade, Chem. Commun. 792 (1971).

[38] E. D. Jemmis, M. M. Balakrishnarajan, and P. D. Pancharatna, J. Am. Chem. Soc. **123**, 4313 (2001).

[39] A. J. Welch, Chem. Commun. **49**, 3615 (2013).

[40] C. P. Priyakumari and E. D. Jemmis, in *The Chemical Bond* (Wiley-VCH, Weinheim, 2014), p. 113.

[41] E. D. Jemmis and D. L. V. K. Prasad, J. Solid State Chem. **179**, 2768 (2006).

[42] H. Werheit, Phys. Rev. Lett. **118**, 089601 (2017).

[43] Q. An, K. M. Reddy, K. Y. Xie, K. J. Hemker, and W. A. Goddard, Phys. Rev. Lett. **118**, 089602 (2017).

[44] T. Ogitsu, V. Lordi, E. Schwegler, and M. Widom, Phys. Rev. Lett. **118**, 159601 (2017).

[45] Q. An, K. M. Reddy, K. Y. Xie, K. J. Hemker, and W. A. Goddard, Phys. Rev. Lett. **118**, 159902 (2017).